Scientia Iranica, Vol. 12, No. 4, pp 329–337
© Sharif University of Technology, October 2005

SCIENTIA IRANICA

Axisymmetric Radial Stagnation-Point Flow of a Viscous Fluid on a Rotating Cylinder with Time-Dependent Angular Velocity

R. Saleh[1] and A.B. Rahimi*

The unsteady viscous flow in the vicinity of an axisymmetric stagnation point of an infinitely long rotating circular cylinder is investigated, when the angular velocity varies arbitrarily with time. The free stream is steady and with a constant strain rate of k. An exact solution of the Navier-Stokes equations is derived in this problem. The general self-similar solution is obtained when the angular velocity of the cylinder varies as certain functions. The cylinder may perform different types of motion: It may rotate with constant speed, with exponentially increasing/decreasing angular velocity, with harmonically varying rotation speed or with accelerating/decelerating oscillatory angular speed. For completeness, some sample semi-similar solutions of the unsteady Navier-Stokes equations have been obtained numerically using a finite-difference scheme. These solutions are presented for special cases when the time-dependent is step-function, linear and non-linear, with respect to time. All the solutions above are presented for Reynolds numbers, $\mathrm{Re} = ka^2/2v$, ranging from 0.1 to 1000, where a is the cylinder radius and v is the kinematic viscosity of the fluid. Shear stresses corresponding to all cases increase with the Reynolds number. The maximum value of the shear-stress increases with an increase in oscillation frequency and amplitude. An interesting result is obtained, in which a cylinder, spun up from rest with a certain angular velocity function and at a particular value of Reynolds number, is azimuthally stress-free.

INTRODUCTION

The problem of finding exact solutions to Navier-Stokes equations is a very difficult task. This is primarily due to the fact that these equations are nonlinear. However, it is possible to find exact solutions to Navier-Stokes equations in certain particular cases. An exact solution to these equations governing the problem of a two-dimensional stagnation flow against a flat plate has been given by Hiemenz [1]. Later, Homann [2] derived an exact solution to Navier-Stokes equations for the three-dimensional case of an axisymmetric stagnation flow against a plate. Howarth [3] and Davey [4] presented results to unsymmetrical cases of the stagnation flow against a flat plate. The first exact solution to the problem of an axisymmetric stagnation flow on an infinite circular cylinder was obtained by Wang [5]. Gorla [6-9], in a series of papers, studied the steady and unsteady flows over a circular cylinder in the vicinity of the stagnation-point for the cases of constant axial movement and in the special case of the harmonic motion of a non-rotating cylinder. In more recent years, Cunning, Davis and Weidman [10] have considered the stagnation flow problem on a rotating circular cylinder with constant angular velocity, including, also, the effects of suction and blowing in their study. Takhar, Chamkha and Nath [11] have investigated unsteady viscous flow in the vicinity of the axisymmetric stagnation point of an infinite circular cylinder in the particular case when both the cylinder and the free stream velocities vary inversely with time. A study considered by Rahimi [12] presents a systematic solution of Gorla's results for high Prandtl number fluids, using inner-outer expansion of fluid properties.

The effects of cylinder rotation with time-dependent angular velocity, perhaps of especial interest in industrial cooling and centrifugal processes, have not yet been investigated.

In the present analysis, unsteady viscous flow in the vicinity of the axisymmetric stagnation point of

1. *Department of Engineering, Ferdowsi University of Mashhad, Mashhad, I.R. Iran.*
*. *Corresponding Author, Department of Engineering, Ferdowsi University of Mashhad, Mashhad, I.R. Iran.*

an infinite rotating cylinder is considered, when the angular velocity varies arbitrarily with time. An exact solution to the Navier-Stokes equations is obtained. The general self-similar solution is obtained when the angular velocity of the cylinder varies due to certain types of function. The cylinder may perform different types of motion: It may rotate with constant speed, with exponentially increasing/decreasing angular velocity, with harmonically varying rotation speed or with accelerating/decelerating oscillatory angular speed.

The results for different values of the azimuthal component of velocity and shear stresses are presented for Reynolds numbers ranging from 0.1 to 1000. Particular cases of these results are compared with the existing results of Wang [5] and Cunning, Davis and Weidman [10], correspondingly. For completeness, some sample semi-similar solutions of the Navier-Stokes equations are obtained and the results for a few examples of cylinder rotation in the form of step-function, linear and non-linear, with respect to time, are presented for different values of flow parameters.

PROBLEM FORMULATION

The laminar unsteady incompressible flow of a viscous fluid in the neighborhood of an axisymmetric stagnation-point of an infinite rotating circular cylinder is considered. The flow configuration is shown in Figure 1, with cylindrical coordinates (r, θ, z) and with associate velocity components (u, v, w).

The cylinder rotates with time-dependent angular velocity. A radial external flow of strain rate, k, impinges on the cylinder of radius a and is centered at $r = 0$. The unsteady Navier-Stokes equations, with cylindrical polar coordinates governing the axisymmetric flow, are given by [5,7,9]:

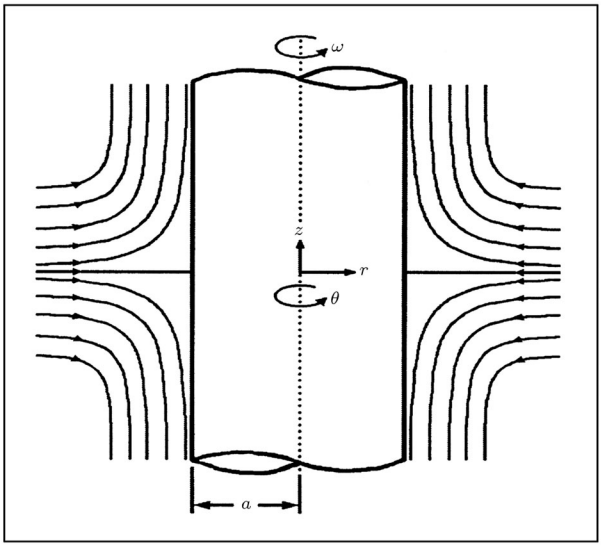

Figure 1. Schematic diagram of a rotating cylinder under radial stagnation flow in the fixed cylindrical coordinate system (r, θ, z).

Mass:

$$\frac{\partial u}{\partial r}(ru) + r\frac{\partial w}{\partial z} = 0. \tag{1}$$

Momentum:

$$\frac{\partial u}{\partial t} + u\frac{\partial u}{\partial r} - \frac{v^2}{r} + w\frac{\partial u}{\partial z} = -\frac{1}{\rho}\frac{\partial p}{\partial r} + \upsilon\left(\frac{\partial^2 u}{\partial r^2} + \frac{1}{r}\frac{\partial u}{\partial r} - \frac{u}{r^2} + \frac{\partial^2 u}{\partial z^2}\right), \tag{2}$$

$$\frac{\partial v}{\partial t} + u\frac{\partial v}{\partial r} + \frac{uv}{r} + w\frac{\partial v}{\partial z} = \upsilon\left(\frac{\partial^2 v}{\partial r^2} + \frac{1}{r}\frac{\partial v}{\partial r} - \frac{v}{r^2} + \frac{\partial^2 v}{\partial z^2}\right), \tag{3}$$

$$\frac{\partial w}{\partial t} + u\frac{\partial w}{\partial r} + w\frac{\partial w}{\partial z} = -\frac{1}{\rho}\frac{\partial p}{\partial z} + \upsilon\left(\frac{\partial^2 w}{\partial r^2} + \frac{1}{r}\frac{\partial w}{\partial r} + \frac{\partial^2 w}{\partial z^2}\right), \tag{4}$$

where p, ρ and υ are the thermodynamic pressure, density and kinematic viscosity, respectively. The boundary conditions for the velocity field are:

$$r = a : u = 0, \qquad v = a.\omega(t), \qquad w = 0, \tag{5}$$

$$r \to \infty : u = -k\left(r - \frac{a^2}{r}\right), \quad \lim_{r\to\infty} rv = 0, \quad w = 2kz. \tag{6}$$

Here, Relations 5 represent no-slip boundary conditions on the cylinder wall, where $\omega(t)$ is the angular velocity of the cylinder. Relations 6 result from the assumption that the viscous flow solution approaches, in a manner analogous to the Hiemenz flow, the potential stagnation field as $r \to \infty$ [10]. The presence of the stagnation flow allows the condition of zero circulation at infinity to be imposed on the swirl velocity.

A reduction of the Navier-Stokes equations is obtained by applying the following transformations:

$$u = -k\frac{a}{\sqrt{\eta}}f(\eta), \quad v = \frac{a}{\sqrt{\eta}}G(\eta, \tau),$$

$$w = 2kf'(\eta)z, \qquad p = \rho k^2 a^2 P, \tag{7}$$

where $\tau = 2kt$ and $\eta = (r/a)^2$ are the dimensionless time and radial variables. The transformations (Equations 7) satisfy Equation 1 automatically and their insertion into Equations 2 to 4 yields a system of differential equations in terms of $f(\eta)$ and $G(\eta, \tau)$ and an expression for the pressure:

$$\eta f''' + f'' + \mathrm{Re}[1 - (f')^2 + ff''] = 0, \tag{8}$$

$$\eta G'' + \mathrm{Re}[fG' - \frac{\partial G}{\partial \tau}] = 0, \tag{9}$$

$$P - P_o = -\left[\frac{f^2}{2\eta} + \frac{1}{\mathrm{Re}} f' + 2\left(\frac{z}{a}\right)^2 - \frac{1}{2k^2}\int_1^\eta \frac{G^2(\xi)}{\xi^2} d\xi\right]. \tag{10}$$

In these equations, primes indicate differentiation with respect to η and $\mathrm{Re} = ka^2/2\upsilon$ is the Reynolds number. From Relations 5 and 6, the boundary conditions for Equations 8 and 9 are as follows:

$$\eta = 1 : f = 0, \quad f' = 0, \quad G = \omega(\tau),$$

$$\eta \to \infty : f' = 1, \quad G = 0. \tag{11}$$

Here, Equations 8 and 9 are for different forms of $\omega(\tau)$ functions and have been solved numerically with Re as the parameter. In what follows, first, the self-similar equations and the exact solutions of some particular $\omega(\tau)$ functions are presented and, then, for completeness, the semi-similar equations and their numerical solutions are presented for a few examples of $\omega(\tau)$ functions.

SELF-SIMILAR EQUATIONS

Equation 9 can be reduced to an ordinary differential equation if one assumes that the function $G(\eta, \tau)$ in Equation 9 is separable as:

$$G(\eta, \tau) = g(\eta).\phi(\tau). \tag{12}$$

Substituting this separation of variables into Equation 9, gives:

$$\eta \frac{g''}{g} + \mathrm{Re}.f\frac{g'}{g} = \frac{\mathrm{Re}}{\phi(\tau)}\frac{d\phi(\tau)}{d\tau}. \tag{13}$$

In Equation 13, both sides must be equal to a constant, hence, the general solution to the differential equation in Equation 13, with τ as an independent variable, is as the following:

$$\phi(\tau) = b.\exp[(\alpha + i\beta)\tau]. \tag{14}$$

Here, $i = \sqrt{-1}$ and b, α and β are constants. Boundary conditions are:

$$G(1, \tau) = \omega(\tau) = \phi(\tau).g(1) \to \phi(\tau) = \omega(\tau),$$

and for $g(1) = 1$ gives:

$$\omega(\tau) = b.\exp[(\alpha + i\beta)\tau],$$

$$G(\infty, \tau) = 0 = \phi(\tau).g(\infty) \to g(\infty) = 0. \tag{15}$$

Substituting the solution in Equation 14 into the differential equation in Equation 13, with η as an independent variable, results in:

$$\eta g'' + \mathrm{Re}[fg' - \alpha g - i\beta g] = 0. \tag{16}$$

Note that in Equations 15, $b = 0$ corresponds to the case of a non-rotating cylinder, as in Wang [5]. If $b \neq 0$ and $\alpha = \beta = 0$, Equations 15 give the case of a rotating cylinder with a constant angular velocity, as in Cunning et al. [10]. If $b \neq 0, \alpha \neq 0$ and $\beta = 0$, Equations 15 give the case of a rotating cylinder with an exponential angular velocity. $b \neq 0, \beta \neq 0$ and $\alpha = 0$ correspond to the case of a pure harmonic rotation of the cylinder. For non-zero b, α and β, Equations 15 give the cases of accelerating and decelerating oscillatory motions of the cylinder.

To obtain solutions to Equation 16, it is assumed that the function $g(\eta)$ is a complex function, such as:

$$g(\eta) = g_1(\eta) + ig_2(\eta). \tag{17}$$

Substituting Equation 17 into Equation 16, the following coupled system of differential equations is obtained:

$$\begin{cases} \eta g_1'' + \mathrm{Re}(fg_1' - \alpha g_1 + \beta g_2) = 0 \\ \eta g_2'' + \mathrm{Re}(fg_2' - \alpha g_2 + \beta g_1) = 0 \end{cases}. \tag{18}$$

Considering the boundary conditions in Relations 5 and 6, the boundary conditions for functions f and g become:

$$\eta = 1 : f = 0, \quad f' = 0, \quad g = 1, \tag{19}$$

$$\eta \to \infty : f' = 1, \quad g = 0. \tag{20}$$

Hence, the boundary conditions on functions g_1 and g_2 are:

$$\eta = 1 : g_1 = 1, \quad g_2 = 0, \tag{21}$$

$$\eta \to \infty : g_1 = 0, \quad g_2 = 0. \tag{22}$$

The coupled Equations 18, along with boundary conditions in Relations 21 and 22, have been solved by using the fourth-order Runge-Kutta method of numerical integration along with a shooting method [13]. Using this method, the initial values of $g_1'(1)$ and $g_2'(1)$ were guessed and the integration was repeated until convergence of the results was reached. The value of $g_2(\eta) = 0$ was assumed initially and, then, by repeating the integration of these two equations, the final values of $g_1(\eta)$ and $g_2(\eta)$ were obtained.

The angular velocity would be described as:

$$\omega(\tau) = b\exp(\alpha\tau)[\cos(\beta\tau) + i\sin(\beta\tau)]. \tag{23}$$

Thus, the azimuthal component of velocity from Equations 7 becomes:

$$v(\eta, \tau) = \frac{ab}{\sqrt{\eta}}\exp(\alpha\tau)[(g_1(\eta)\cos(\beta\tau) - g_2(\eta)\sin(\beta\tau)) + i(g_1(\eta)\sin(\beta\tau) + g_2(\eta)\cos(\beta\tau))]. \tag{24}$$

This component of velocity will be presented for some sample angular velocities in later sections.

PARTIALLY SIMILAR EQUATIONS

Equation 9 may be solved directly for any chosen $\omega(\tau)$ function. The solutions obtained this way are called partially similar solutions. These equations, along with boundary conditions in Relation 11, were solved by using a finite difference method, which lead to a tridiagonal matrix. Assuming steady-state for $\tau \leq 0$, the solution starts from $\omega(0)$ and, marching through time, time-dependent solutions for $\tau \geq 0$ were obtained.

SHEAR-STRESS

The shear-stress at the cylinder surface is calculated from [10]:

$$\sigma = \mu \left[r \frac{\partial}{\partial r}(\frac{v}{r}) \hat{e}_\theta + \frac{\partial w}{\partial r} \hat{e}_z \right], \tag{25}$$

where μ is the fluid viscosity. Using the definitions in Equations 7, the shear-stress at the cylinder surface for semi-similar solutions becomes:

$$\sigma = 2\mu(G'(1,\tau) - \omega(\tau))\hat{e}_\theta + 4\mu \frac{kz}{a} f''(1)\hat{e}_z. \tag{26}$$

Thus, the axial and azimuthal shear stress components are proportional to $f''(1)$, which has been presented in [10] and $(G'(1,\tau) - \omega(\tau))$, respectively. Azimuthal surface shear-stress for self-similar solutions is presented by the following relation:

$$\begin{aligned} \sigma_\theta &= \sigma_{\theta_1} + i\sigma_{\theta_2} \\ &= 2\mu b \exp(\alpha\tau)[\cos(\beta\tau)(g_1'(1)-1) - \sin(\beta\tau) g_2'(1)] \\ &\quad + i(\sin(\beta\tau)(g_1'(1)-1) + \cos(\beta\tau) g_2'(1))], \end{aligned} \tag{27}$$

some numerical values of σ_{θ_1} will be presented later for a few examples of angular velocities.

PRESENTATION OF RESULTS

In this section, the solution results of self-similar Equations 16 and semi- similar Equation 9, along with surface shear stresses for different functions of angular velocity, are presented. Also, the azimuthal component of velocity, $v(\eta,\tau)$, for both cases mentioned above, are given.

Figure 2 represents sample profiles of the $g(\eta)$ function and the azimuthal component of velocity for

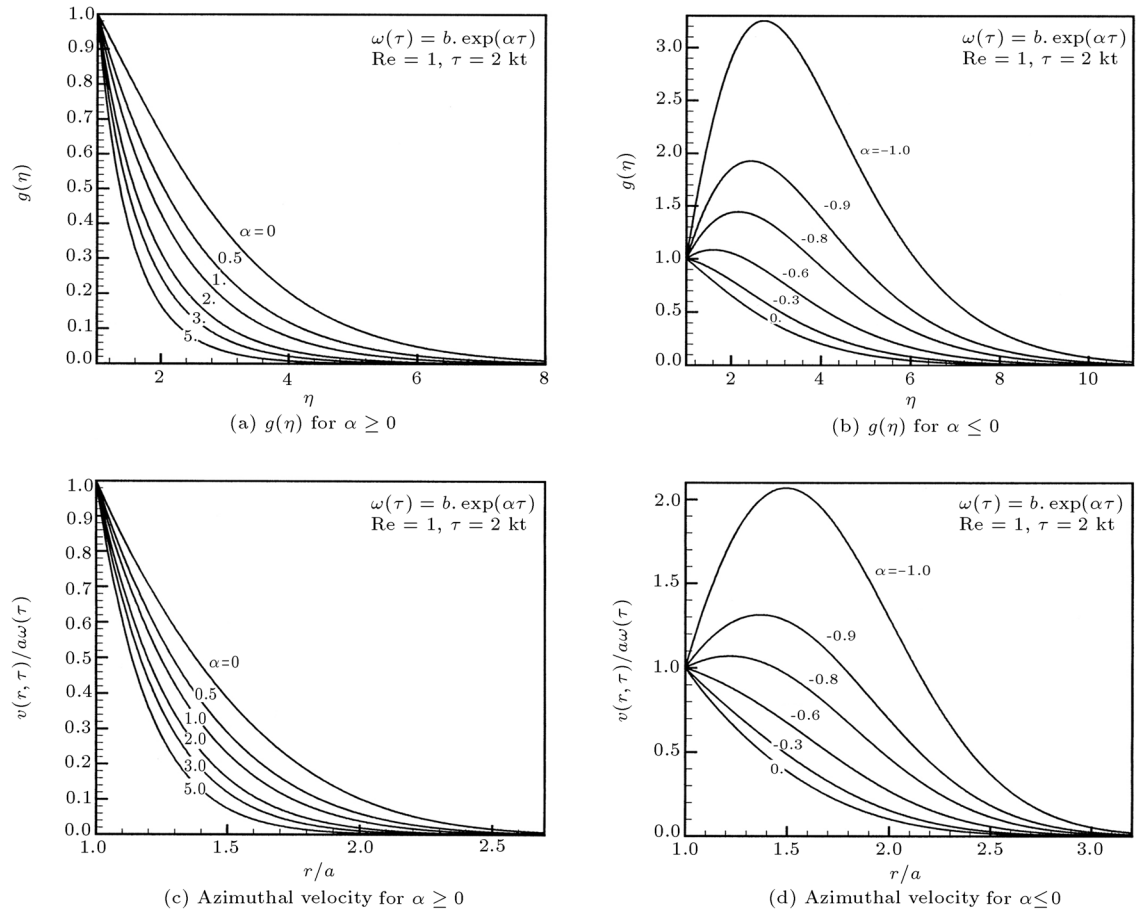

(a) $g(\eta)$ for $\alpha \geq 0$

(b) $g(\eta)$ for $\alpha \leq 0$

(c) Azimuthal velocity for $\alpha \geq 0$

(d) Azimuthal velocity for $\alpha \leq 0$

Figure 2. Sample profiles of $g(\eta)$ and their corresponding azimuthal velocity for cylinder with exponential angular velocity.

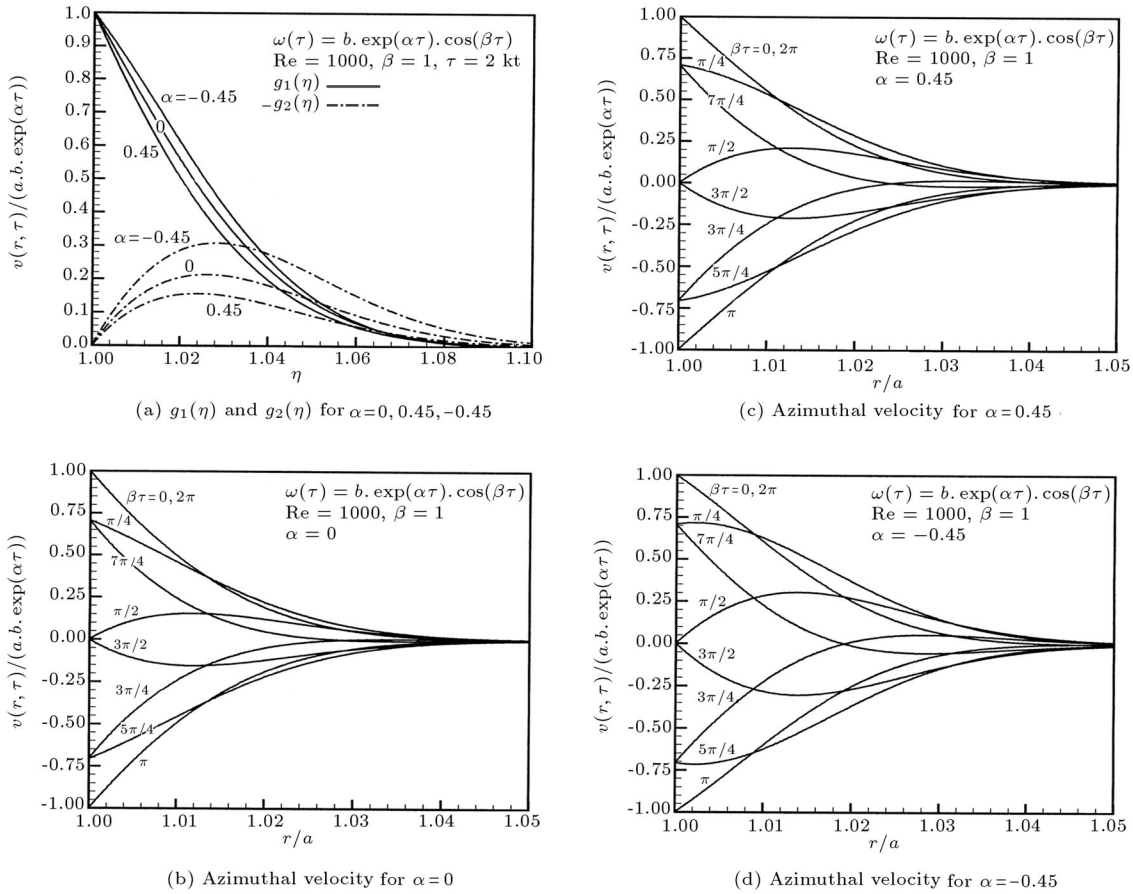

(a) $g_1(\eta)$ and $g_2(\eta)$ for $\alpha = 0, 0.45, -0.45$

(c) Azimuthal velocity for $\alpha = 0.45$

(b) Azimuthal velocity for $\alpha = 0$

(d) Azimuthal velocity for $\alpha = -0.45$

Figure 3. Sample profiles of $g(\eta)$ and their corresponding azimuthal velocity for cylinder with accelerating and decelerating oscillatory motion.

$\omega(\tau)$ in exponential form, for Re = 1. Figures 2a and 2c exhibit the accelerating case and Figures 2b and 2d show the decelerating case. It is interesting to note that for $\alpha \succ 0$, as α increases, the depth of diffusion of the fluid velocity field decreases and, for $\alpha \prec 0$, as the absolute value of α increases, the fluid velocity in the vicinity of the cylinder cannot decrease at the same rate as the cylinder rotation velocity. Therefore, in this region, as the figure shows, fluid velocity is greater than cylinder velocity. Also, $\alpha = 0$ indicates the case of a rotating cylinder with a constant angular velocity [10].

Figure 3 presents sample profiles of the $g(\eta)$ function and the azimuthal component of the velocity when $\omega(\tau)$ represents the accelerating and decelerating oscillatory motion of the cylinder for Re = 1000. Here, the azimuthal velocity component is shown for a complete period of oscillation. Figure 3b is for pure harmonic motion and Figures 3c and 3d present the state of accelerating and decelerating harmonic motion, respectively. Here, as in the exponential angular velocity case, the diffusion depth of the fluid velocity field for $\alpha \succ 0$ and $\alpha \prec 0$ is less, but more than in the case of $\alpha = 0$, respectively.

Figure 4 represents a sample of the $g(\eta)$ function and the azimuthal component of velocity for the harmonic motion of the cylinder in different frequencies and for a complete period of oscillation. Here, the case of $\beta = 0$ is the same as [10] and, as stated in the previous discussion, as β increases, the diffusion depth of the fluid velocity field decreases.

Figure 5 represents the azimuthal shear-stress on the surface of the cylinder with harmonic rotation and with accelerating and decelerating oscillatory motion. This shear-stress is for a complete period between 0 and 2π. From Figure 5a, as the frequency of the oscillation increases, the maximum of the absolute value of the shear-stress increases and $\beta = 0$ corresponds to the case of constant angular velocity (see [10]). Comparing Figures 4b and 5a indicates that shear-stress and azimuthal velocity are in different phases. Figure 5b is for $\alpha = 0$ and indicates the case of pure oscillation. For $\alpha \succ 0$ and $\alpha \prec 0$, the maximum of the absolute value of shear-stress is more, and less than that in the case of pure oscillation, respectively. Also, the phase-difference of shear-stress and azimuthal velocity decreases as α increases.

Figure 6 exhibits the azimuthal shear-stress on

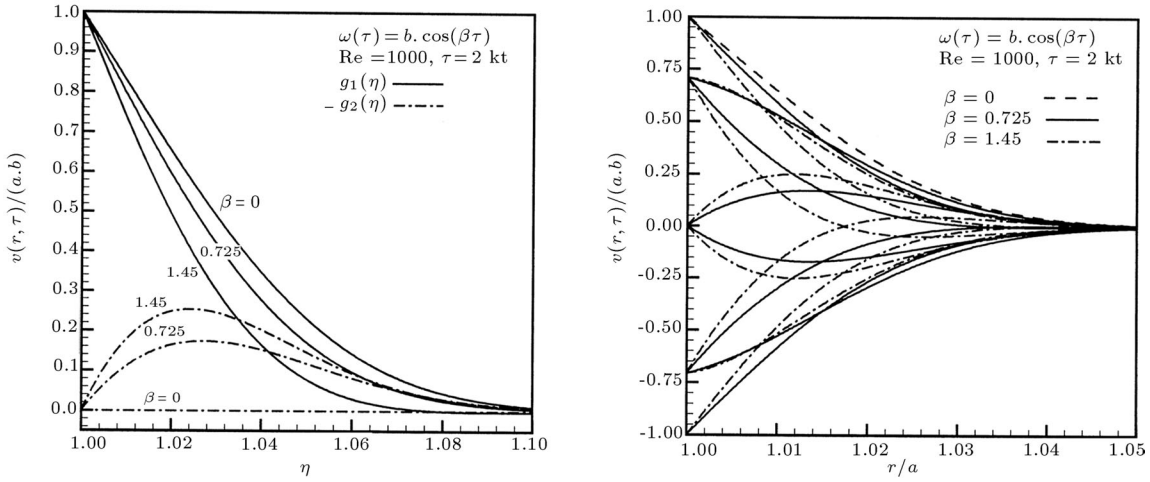

(a) $g_1(\eta)$ and $g_2(\eta)$ (b) Azimuthal velocity

Figure 4. Sample profiles of $g(\eta)$ and their corresponding azimuthal velocity for cylinder with harmonic rotation.

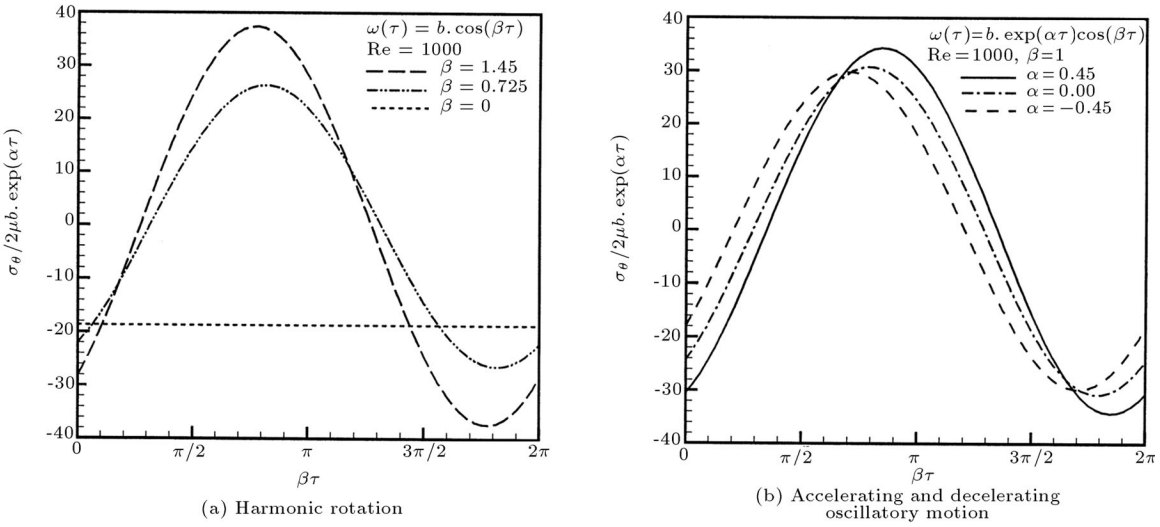

(a) Harmonic rotation (b) Accelerating and decelerating oscillatory motion

Figure 5. Azimuthal shear-stress component for cylinder.

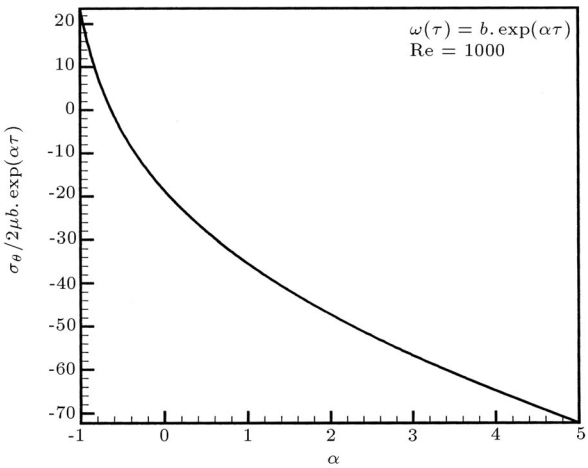

Figure 6. Azimuthal shear-stress component for cylinder with exponential angular velocity.

the surface of the cylinder for an exponential angular velocity with different acceleration. Also, it is seen that the slope of this curve is decreasing as α increases, meaning that the sensitivity of shear-stress, with respect to the variation of α, decreases as α increases and $\alpha = 0$ corresponds to the same shear-stress as the case in [10]. It is interesting to note that for a particular value of α, shear-stress is zero.

Figures 7 to 9 represent the partially similar solutions to different forms of time-dependent angular velocity, including: Step-function, linear and inverse functions, in which function $G(\eta, \tau)$ is shown in terms of η, different time values and Reynolds numbers.

Figure 10 shows the azimuthal shear-stress component on the surface of the cylinder for different time-dependent angular velocities. These angular velocity

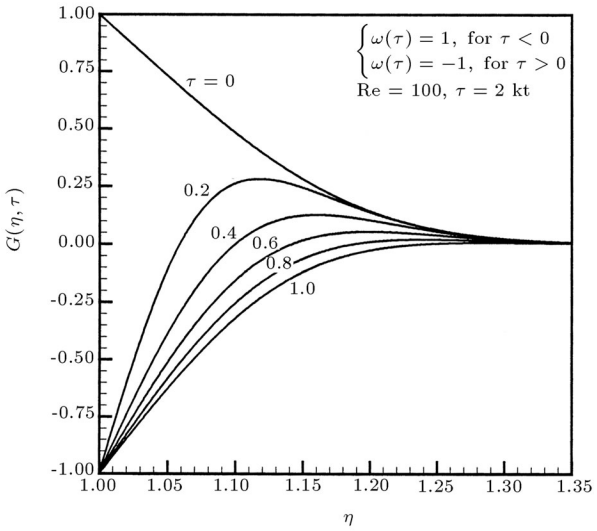

Figure 7. Sample profile of $G(\eta, \tau)$ for cylinder with angular velocity as $\omega(\tau) = 1$ for $\tau \prec 0$ and $\omega(\tau) = -1$ for $\tau \succ 0$.

functions are numbered here, respectively, as in Figure 10:

$$1 - \begin{cases}\omega(\tau) = 0. & \text{for } \tau \prec 0\\ \omega(\tau) = 1. & \text{for } \tau \succ 0\end{cases},$$

$$2 - \begin{cases}\omega(\tau) = 1. & \text{for } \tau \prec 0\\ \omega(\tau) = 0. & \text{for } \tau \succ 0\end{cases},$$

$$3 - \begin{cases}\omega(\tau) = 0. & \text{for } \tau \prec 0\\ \omega(\tau) = \tau. & \text{for } \tau \succ 0\end{cases},$$

$$4 - \begin{cases}\omega(\tau) = 0. & \text{for } \tau \prec 0\\ \omega(\tau) = \tau^2. & \text{for } \tau \succ 0\end{cases},$$

$$5 - \begin{cases}\omega(\tau) = 0. & \text{for } \tau \prec 0\\ \omega(\tau) = \tau^{\frac{1}{2}}. & \text{for } \tau \succ 0\end{cases},$$

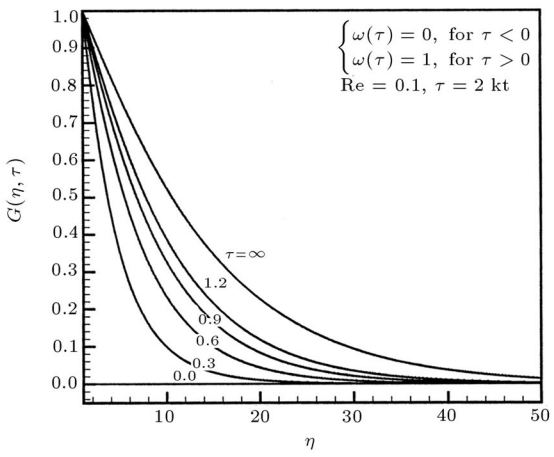

(a) Step-function

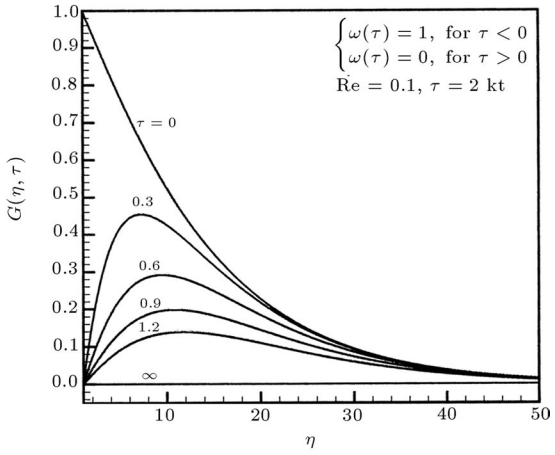

(b) Step-function

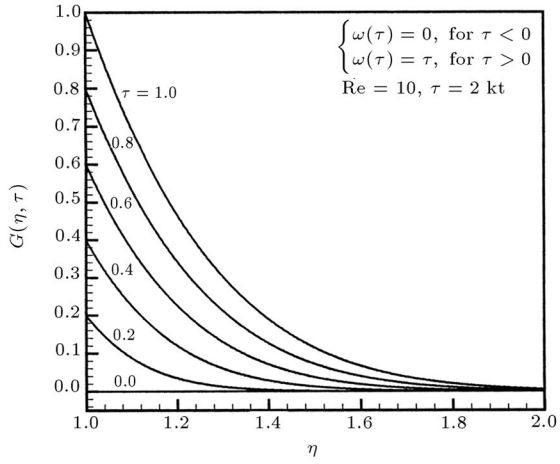

(c) Linear function

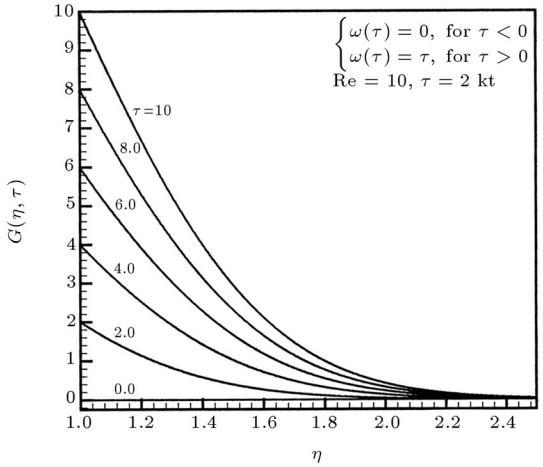

(d) Linear function

Figure 8. Sample profiles of $G(\eta, \tau)$ for different angular velocity functions.

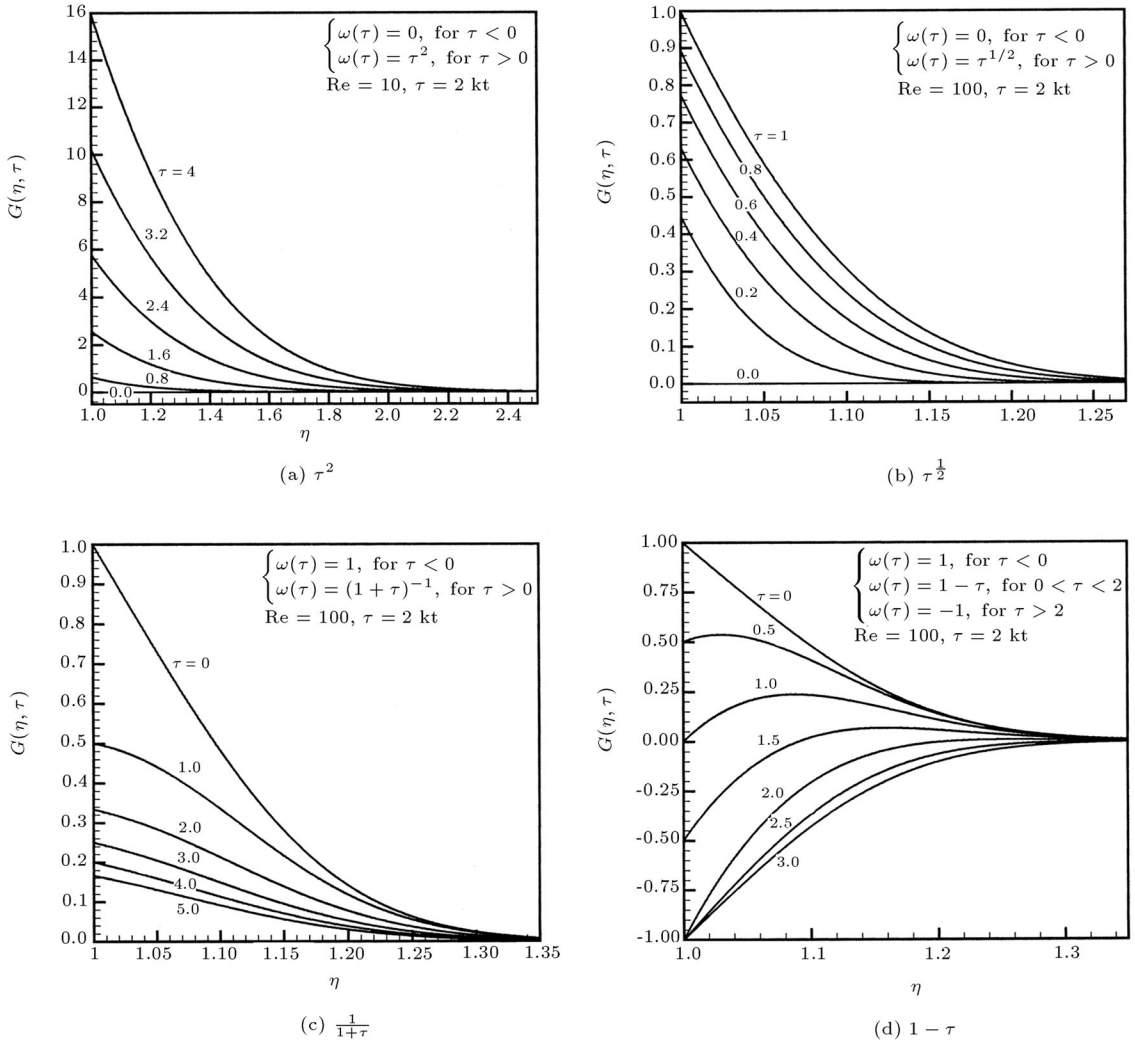

Figure 9. Sample profiles of $G(\eta, \tau)$ for different angular velocity functions.

$$6 - \begin{cases} \omega(\tau) = 1. & \text{for } \tau \prec 0 \\ \omega(\tau) = \frac{1}{1+\tau}. & \text{for } \tau \succ 0 \end{cases},$$

$$7 - \begin{cases} \omega(\tau) = 1. & \text{for } \tau \prec 0 \\ \omega(\tau) = 1 - \tau. & \text{for } 0 \prec \tau \prec 2 \\ \omega(\tau) = -1. & \text{for } \tau \succ 2 \end{cases},$$

$$8 - \begin{cases} \omega(\tau) = 1. & \text{for } \tau \prec 0 \\ \omega(\tau) = -1. & \text{for } \tau \succ 0 \end{cases}$$

Figures 10a and 10b show shear-stress on the surface of the cylinder at Re = 1 and Re = 100, respectively. It is evident from these two figures that the surface shear-stress increases as the Reynolds number increases.

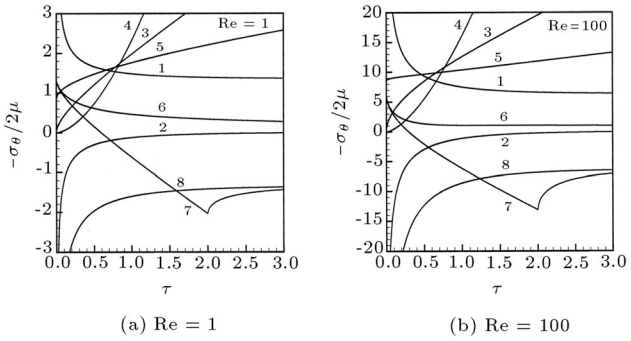

Figure 10. Azimuthal shear-stress component for cylinder with different angular velocity functions.

CONCLUSIONS

An exact numerical solution to the Navier-Stokes equations is obtained for the problem of the stagnation-point flow on a circular cylinder. A general self-similar solution is obtained when the cylinder has different forms of rotational motion, including constant angular velocity rotation, exponential angular velocity rotation, pure harmonic rotation and both accelerating and decelerating oscillatory rotations. Also, some

sample partially similar solutions for the same problem have been considered when the circular cylinder is rotating with different types of time-dependent angular velocity. The azimuthal component of the fluid velocity and surface azimuthal shear-stress on the cylinder are obtained in all the above situations for different values of Reynolds number. The absolute value of azimuthal shear stress, corresponding to all cases, increases with an increase in the Reynolds number. Also, the maximum value of shear-stress increases with an increase in oscillation frequency and acceleration and with the decelerating parameter in the exponential amplitude function. It is also shown that a cylinder spun up from rest in an exponential manner is azimuthally stress-free for certain combinations of Reynolds number and rate of this exponential function.

REFERENCES

1. Hiemenz, K. "Die Grenzchicht an einem in den gleichformingen Flussigkeitsstrom eingetauchten geraden Kreiszylinder", *Dinglers Polytech. J.*, **326**, pp 321-410 (1911).
2. Homann, F.Z. "Der Einfluss grosser Zahighkeit bei der Strmung um den Zylinder und um die Kugel", *Zeitsch. Angew. Math. Mech.*, **16**, pp 153-164 (1936).
3. Howarth, L. "The boundary layer in three dimensional flow", Part II. *The Flow Near a Stagnation Point. Phil. Mag. Series 7*, **42** pp 1433-1440 (1951).
4. Davey, A. "Boundary layer flow at a saddle point of attachment", *Journal of Fluid Mechanics*, **10**, pp 593-610 (1951).
5. Wang, C. "Axisymmetric stagnation flow on a cylinder", *Quarterly of Applied Mathematics*, **32**, pp 207-213 (1974).
6. Gorla, R.S.R. "Unsteady laminar axisymmetric stagnation flow over a circular cylinder", *Dev. Mech.*, **9**, pp 286-288 (1977).
7. Gorla, R.S.R. "Nonsimilar axisymmetric stagnation flow on a moving cylinder", *Int. J. Engineering Science*, **16**, pp 392-400 (1978).
8. Gorla, R.S.R. "Transient response behaviour of an axisymmetric stagnation flow on a circular cylinder due to a time dependent free stream velocity", *Lett. Appl. Engineering Science*, **16**, pp 493-502 (1978).
9. Gorla, R.S.R. "Unsteady viscous flow in the vicinity of an axisymmetric stagnation-point on a cylinder", *Int. J. Engineering Science*, **17**, pp 87-93 (1979).
10. Cunning, G.M., Davis, A.M.J. and Weidman, P.D. "Radial stagnation flow on a rotating cylinder with uniform transpiration", *Journal of Engineering Mathematics*, **33**, pp 113-128 (1998).
11. Takhar, H.S., Chamkha, A.J. and Nath, G. "Unsteady axisymmetric stagnation-point flow of a viscous fluid on a cylinder", *Int. Journal of Engineering Science*, **37**, pp 1943-1957 (1999).
12. Rahimi, A.B. "Heat transfer in an axisymmetric stagnation flow on a cylinder at high Prandtl numbers using perturbation techniques", *Int. J. of Engr. Science*, **10**(3), Iran Univ. of Science & Tech. (1999).
13. Press, W.H., Flannery, B.P., Teukolsky, S.A. and Vetterling, W.T., *Numerical Recipes, the Art of Scientific Computing*, Cambridge University Press, Cambridge (1997).